JOURNAL OF SOLID STATE CHEMISTRY 92, 339–351 (1991)

$BaNdCe_{0.9}Fe_{1+x}Cu_{1-x}O_{7-\delta}$: An Intergrowth of the $BaYFeCuO_5$ Type and CeO_2 Fluorite Type Structures

C. MICHEL,* M. HERVIEU, AND B. RAVEAU

Laboratoire CRISMAT-ISMRa Bd du Maréchal Juin, 14050 Caen Cedex, France

Received November 26, 1990; in revised form January 18, 1991

A new layered copper oxide $BaNdCe_{0.9}Fe_{1.1}Cu_{0.9}O_{7-\delta}$ has been isolated. Its tetragonal structure (a = 3.902 Å, c = 20.895 Å) has been studied by X-ray powder diffraction and HREM. This oxide can be described as an intergrowth of the $NdBaFeCuO_5$ structure (isostructural with $YBaFeCuO_5$) and the CeO_2 fluorite structure. Thus it belongs to a series of oxides, characterized by double fluorite layers, resulting from the introduction of one additional $[CeO_2]_\infty$ fluorite layer in mother structures involving double pyramidal copper layers $[A_2Cu_2O_5]_\infty$. The systematic HREM study of samples of nominal compositions "$BaNdCe_{0.9}Fe_{1.1}Cu_{0.9}O_7$" and "$BaNdCeFeCuO_7$" shows, besides regular crystals, extended intergrowth defects, i.e., mainly single fluorite-layered defects leading to intergrowths $[NdBaFeCuO_5]_m$ $[Ln_2BaFeCuO_7]_n$, triple fluorite-layered defects leading to possible intergrowths $[Ln_3BaFeCuO_9]_m$ $[Ln_2BaFeCeO_7]_n$, and triple perovskite-layered defects suggesting the existence of possible intergrowths $[Ba_2Ln_2(Fe,Cu)_3O_{9+\delta}]_m$ $[Ln_2BaFeCuO_7]_n$. More complex intergrowth defects (multiple fluorite and perovskite layers, superdislocations) are also observed. These observations suggest that the systematic investigation of similar systems should allow complex disordered and ordered intergrowths $[A_2Cu_2O_5]^P_h[ACuO_{3-x}]^P_i[LnO_2]^F_j[A'O]^{RS}_k$ to be isolated.

Consideration of the layered copper oxides $(A_2Cu_2O_5)^P$ $(A'O)^{RS}_n$, whose structure corresponds to the intergrowth of oxygen-deficient double perovskite layers with multiple rock salt layers, shows that these compounds exhibit a great similarity with the fluorite structure. One indeed observes that the A cations (Y, Ca) which are interleaved between the pyramidal copper layers (Fig. 1a) form a single layer of edge-sharing AO_8 cubes similar to those encountered in the fluorite structure. Starting from this analogy between the two structures, it is possible to generate new structures involving double fluorite type layers interleaved between two pyramidal copper layers (Fig. 1b). The oxides $Tl_{1-x}A_{2-y}Ln_2Cu_2O_9$ (Ln = Pr, Nd, Ce) (*1*) and $Nd_{2.64}Sr_{0.82}Ce_{0.54}Cu_2O_8$ (*2*), which were first synthesized almost simultaneously, support this viewpoint. The structure of the first one is derived from that of $TlBa_2CaCu_2O_7$ by replacing the $[CaO_2]_\infty$ single fluorite layer by a $[Pr_2O_4]_\infty$ double fluorite layer leading to the ideal formula $TlBa_2Pr_2Cu_2O_9$. In the same way, the second one called T* corresponds to the replacement of a $[CaO_2]_\infty$ layer in the $La_2CaCu_2O_6$ type structure, by a double fluorite type layer $[(Nd, Ce)_2O_4]_\infty$. The analogous replacement of single by double fluorite type layers in $Bi_2Sr_2CaCu_2O_8$ and $Tl_2Ba_2CaCu_2O_8$ leads to the oxides $Bi_2Sr_2Ln_{2-x}Ce_xCu_2O_{10}$

* To whom correspondence should be addressed.

0022-4596/91 $3.00

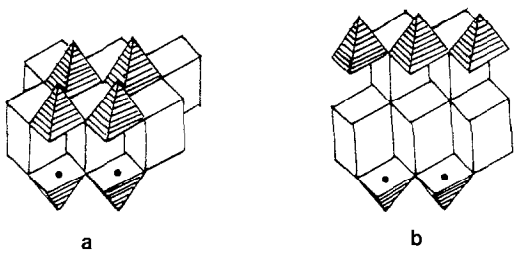

FIG. 1. AO_8 cubes (a) and double fluorite-type layer (b) interleaved between two pyramidal copper layers.

and $Tl_2Ba_2Ln_{2-x}Ce_xCu_2O_{10}$ (*3*), whereas $Pb_2Sr_2LnCeCu_3O_{10+\delta}$ (*4*) is derived from $Pb_2Sr_2Ca_{0.5}Y_{0.5}Cu_3O_8$ by replacing a $[Ca_{0.5}Y_{0.5}O_2]$ layer by a $[(Ln, Ce)_2O_4]_\infty$ layer. This possibility of introduction of additional fluorite layer is not limited to the intergrowth family, but is also observed for the oxygen-deficient perovskite $YBa_2Cu_3O_7$, in which the replacement of the $[YO_2]_\infty$ layer by a double fluorite layer $[(Ln, Ce)_2O_4]_\infty$ leads to the oxides $(Ln_{1-x}Ce_x)_2(Ba_{1-y}Ln_y)_2Cu_3O_9$ (*5, 6*). This suggests that it should be possible to generate a new structure characterized by double fluorite type layers from every oxide which exhibits double pyramidal copper layers $[A_2Cu_2O_5]_\infty$. Among the different layered cuprates, which have been isolated up to now, $YBaFeCuO_5$ (*7*) is also a good candidate. Nevertheless yttrium is not really favorable for the generation of fluorite structure contrary to neodymium and cerium. For this reason the system Nd–Ce–Ba–Fe–Cu–O was investigated. The present paper deals with the synthesis and structural study of a new member of the "double fluorite family," $BaNdCe_{0.9}Fe_{1+x}Cu_{1-x}O_{7-\delta}$.

Experimental

Samples were prepared in air by solid state reaction between barium carbonate and the oxides Nd_2O_3, CeO_2, Fe_2O_3, and CuO. Adequate mixtures of the reactants were intimately ground, pressed into pellets, heated in alumina crucibles at 1000°C for 48 hr and then quenched down to room temperature.

X-ray diffraction data were collected by step scanning over an angular range of $10° \leq 2\Theta \leq 100°$ in increments of 0.02° (2Θ) by means of a Philips diffractometer using the Cu$K\alpha$ radiation. The Bragg reflections were used to refine the cell parameters and the crystal structure with the profile refinement computer program DBW 3.2 (*8*).

The electron diffraction and electron microscopy studies were performed with a JEOL 120 CX electron microscope fitted with a side entry goniometer (±60°). The high resolution study was performed with a JEOL 200 CX electron microscope (200 kV, Cs = 0.8 mm).

Results and Discussion

Numerous compositions close to the stoichiometric formula $NdCeBaFeCuO_7$ which corresponds to the ideal structure of the 1 : 1 intergrowth of $BaNdFeCuO_5$ with CeO_2 were investigated, varying Fe/Cu, Nd/Ce, and Nd/Ba molar ratios. Series of annealings at different temperatures and grinding between the different steps were performed in order to isolate pure phases. A pure phase could only be obtained for the composition $NdCe_{0.9}BaFe_{1.1}Cu_{0.9}O_{7-\delta}$. All the attempts for other compositions were unsuccessful. It is worth pointing out that for the ideal composition $CeNdBaFeCuO_7$, besides the X-ray pattern of the expected phase one always observes very weak extra lines which are attributed to CeO_2.

The electron diffraction study of the pure phase shows that it exhibits a tetragonal symmetry with reflection conditions *hkl*, $h + k + l = 2n$ in agreement with the expected structural model for this oxide. This allowed the X-ray powder pattern to be indexed in a tetragonal cell with the following parameters.

$a = 3.9025(1)$ Å and $c = 20.8955(5)$ Å.

TABLE I

$BaNdCe_{0.9}Fe_{1.1}Cu_{0.9}O_7$, SPACE GROUP *I4/mmm*

Atom	Site	*x/a*	*y/b*	*z/c*	*B* (Å^2)
Ba	2*b*	0.0	0.0	0.5	1.4(1)
Nd, Ce	4*c*	0.0	0.0	0.3124(1)	0.0(1)
Fe, Cu	4*c*	0.0	0.0	0.0976(2)	1.0(1)
O(1)	2*a*	0.0	0.0	0.0	0.4(5)
O(2)	8*g*	0.0	0.5	0.1124(6)	2.0(3)
O(3)	4*d*	0.0	0.5	0.25	1.3(4)

Note. a = 3.9025(1) Å c = 20.8955(5) Å; angular range, $10° < 2\Theta < 100°$; $R_p = 0.089$, $R_{wp} = 0.114$, $R_{exp} = 0.113$, $R_i = 0.046$; $N\text{-}P + C = 4481$, $N_{hkl} = 72$.

Structure Determination: X-Ray Diffraction and HREM Study

The starting model was derived from the structure of $YBaFeCuO_5$ (*7*) in which a single fluorite type layer $[YO_2]_\infty$ is replaced by a double fluorite type layer $[NdCeO_4]_\infty$. No ordering between copper and iron or between neodymium and cesium was considered owing to the very close scattering factors of the corresponding elements. Taking into consideration the partial occupation of the fluorite type sites, according to the formula $BaCe_{0.9}NdCu_{0.9}Fe_{1.1}O_{7-\delta}$, the calculations were performed in the space group *I4/mmm*. Taking into consideration the charge balance and the structural model, the maximum of the oxygen content deviation is 0.05; the oxygen content was then fixed to 7. The cell parameters, atomic coordinates, and isotropic thermal factors were refined for the metallic and oxygen atoms successively. The lowest R values ($R_p = 0.089$, $R_i = 0.46$) were obtained for the final parameters given in Table I. Experimental, calculated, and difference X-ray diffraction powder patterns (Fig. 2) attest to the validity of the proposed structural model (Fig. 3). The structure of this phase can indeed be described as an intergrowth of double oxygen-deficient perovskite layers of the $BaYFeCuO_5$ type with single fluorite type layers, forming then double fluorite layers

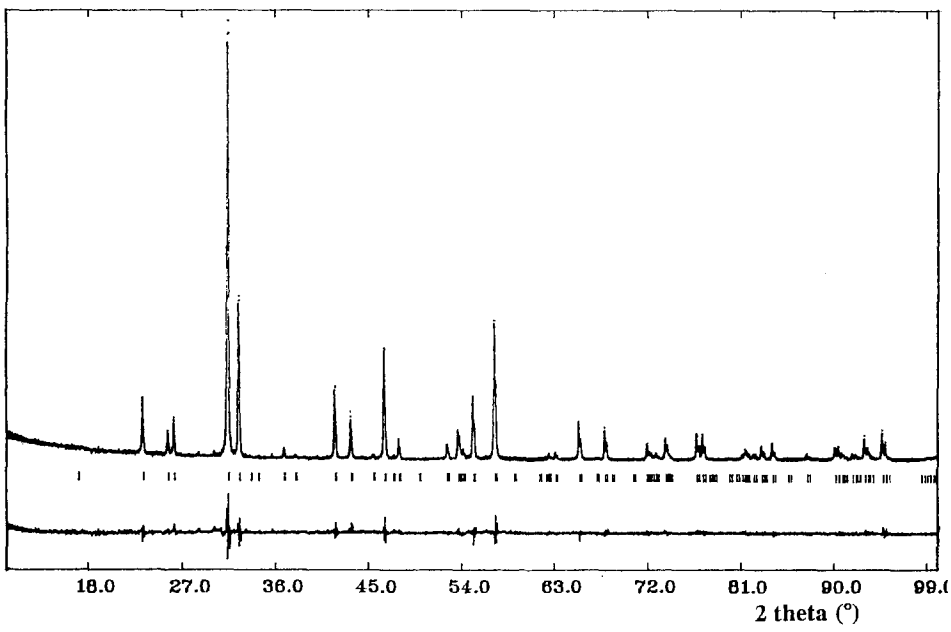

FIG. 2. Experimental, calculated and difference X-ray diffraction powder patterns for $BaNdCe_{0.9}Fe_{1.1}Cu_{0.9}O_7$.

TABLE II

INTERATOMIC DISTANCES (IN Å)

Ba–O(1)	2.76 × 4	Fe, Cu–O(1)	2.04 × 1
Ba–O(2)	3.05 × 8	Fe, Cu–O(2)	1.97 × 4
(Nd, Ce)–O(2)	2.51 × 4		
(Nd, Ce)–O(3)	2.35 × 4		

interleaved between two pyramidal copper/iron layers.

This structural model is confirmed by high resolution electron microscopy, as illustrated in Fig. 4 where the cation positions are highlighted. The contrast consists of one double row of alternating bright dots, correlated to the Nd and Ce layers, and a single row of bright dots, correlated to the barium layers; between these rows are located single rows of small dots correlated to the $[(Cu, Fe)O_2]_\infty$ layers.

The interatomic distances (Table II) are compatible with the radii of the elements and close to those observed in $YBaFeCuO_5$. In particular, the apical distance (Fe, Cu)–O in the $(Fe, Cu)O_5$ square-based pyramids (2.04 Å) does not greatly differ from those calculated in the latter (2.00 and 2.13 Å). This distance is considerably shorter than those observed in superconducting oxides with copper in a pyramidal coordination which are generally greater than 2.30 Å (*9*).

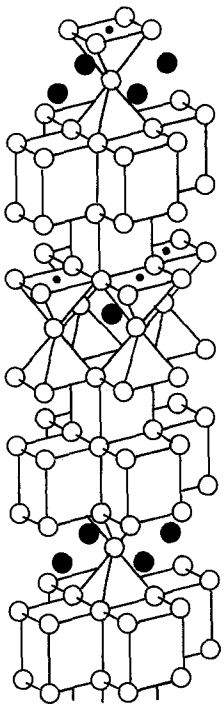

FIG. 3. Perspective view of the structure of the oxide $BaNdCe_{0.9}Fe_{1.1}Cu_{0.9}O_7$: oxygen atoms are symbolized by open circles, iron and copper by small black circles, and barium by large black circles.

Extended Defects: Complex Intergrowth Phenomena

A systematic investigation by high resolution electron microscopy was performed on two samples of nominal composition $BaCe_{0.9}NdCu_{0.9}Fe_{1.1}O_{7-\delta}$ and $BaCeNdCuFeO_7$. The first type of samples, which are obtained as a pure phase from X-ray diffraction characterization, exhibits a large majority of crystals which are free of defects. In contrast, for the second type of samples, which would correspond to the ideal formula but corresponds to a mixture of this new phase with CeO_2, one observes a great number of extended defects in the crystals. Most of the defects are related to variations in the stacking of the perovskite (P) and fluorite (F) layers.

The nature of the extended defects was deduced from the periodicity of the new slice, their shifting with respect to adjacent layers, and from the contrast observed through the focus series where the different types of layers can be lighted.

(*i*) *Single fluorite layered defects: Disordered intergrowths* $[NdBaFeCuO_5]_m[NdCeBaFeCuO_7]_n$. The most frequent defect which affects the fluorite layers deals with the existence of single fluorite layers, (SF) as shown in Fig. 5a. On this image, the double rows of white dots correspond to the copper layers which are separated either by

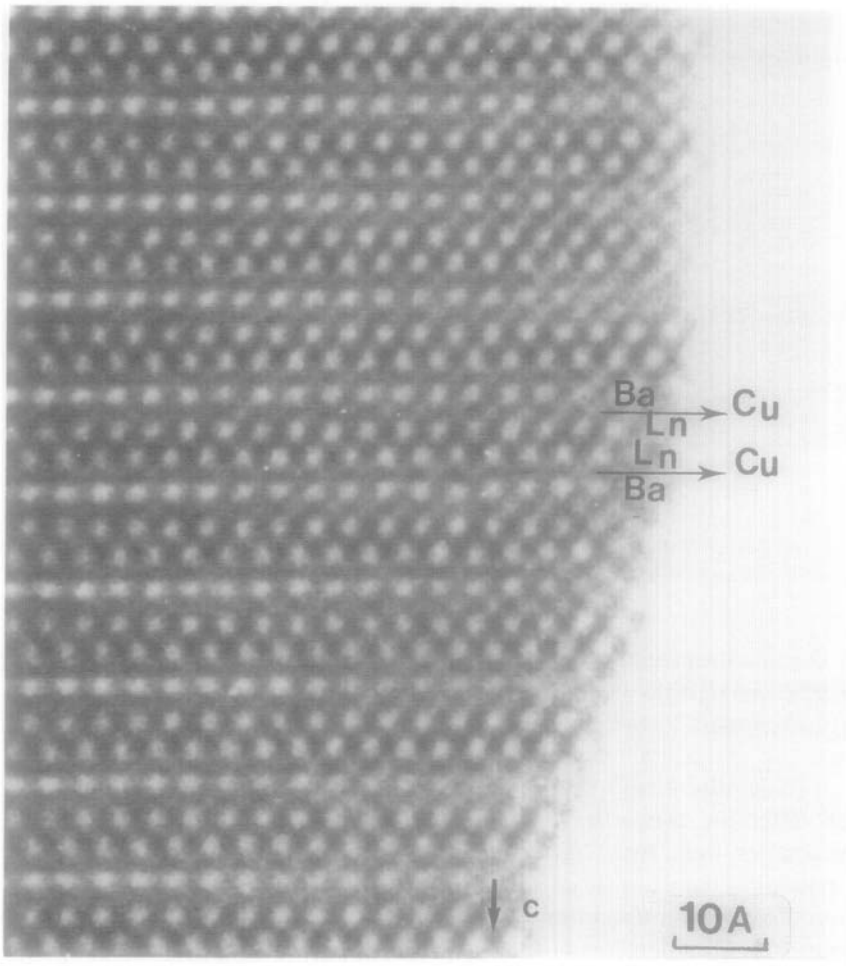

FIG. 4. A [010] high resolution image showing the layers stacking in $NdCe_{0.9}BaFe_{1.1}Cu_{0.9}O_7$.

a single row or by a double row of small dots correlated to the $[BaO]_\infty$ or the $[NdCe]_\infty$ layers, respectively. At the level of the defects (arrowed), the double rows $[NdCe]_\infty$ are replaced by a single row $[Nd]_\infty$ and the shifting of the copper layers has disappeared, in agreement with the appearance of a single fluorite layer (Fig. 5b). Such a slice corresponds to the occurence of the oxygen-deficient perovskite $NdBaFeCuO_5$ (10) in the matrix.

The "SF" defective layers are generally isolated but they can sometimes occur in the form of local intergrowth with the double fluorite layers (Fig. 6a) or of extended domains (Figure 6b). In the first case (Fig. 6a) the double fluorite layers appear as double rows of alternating white dots whereas the single layers correspond to the $[Nd]_\infty$ layers. It can be seen that the two sorts of fluorite slices $[NdCeO_4]_\infty$ and $[NdO_2]_\infty$ are distributed in an aleatory way so that we obtain a "disordered" intergrowth of the two structures, $NdBaFeCuO_5$ type and $NdCeBaFeCuO_7$ type, according to the formula $[NdBaFeCuO_5]_m$ $[Ln_2BaFeCuO_7]_n$ (Ln =

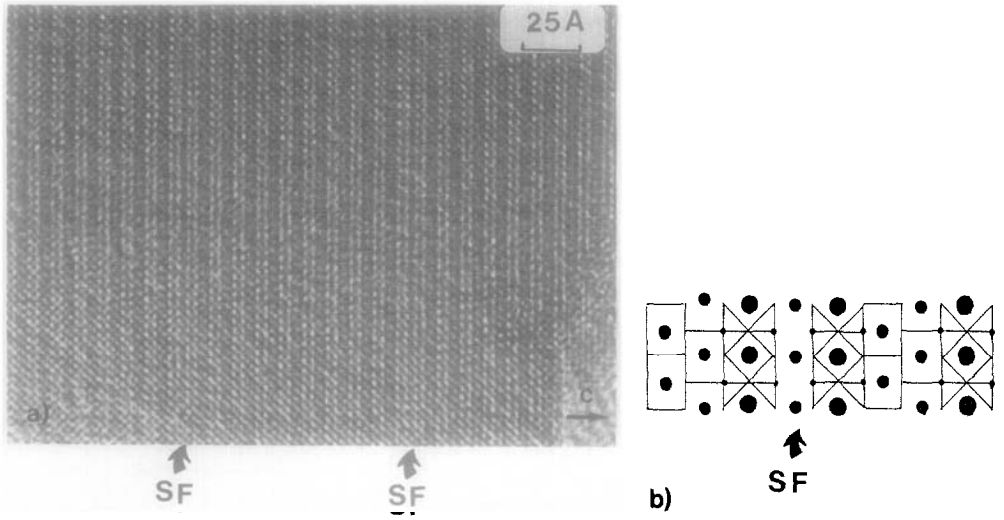

FIG. 5. (a) Defective layers (arrowed) corresponding to the existence of single fluorite layers (SF) are observed in the matrix. (b) Idealized model of the defect.

Nd, Ce). On this latter image the sequence is: ‖4‖2‖1‖1‖5‖1‖3‖1‖1‖2‖1‖, where the normal numbers correspond to m [$NdBaFeCuO_5$] layers, and the underlined numbers correspond to n [$NdCeBaFeCuO_7$] type layers.

In such defective areas the m value is generally smaller than two. Nevertheless, in some regular crystals, a large slice with higher m value can be sometimes observed as shown in Fig. 6b where $m = 4$.

(ii) Multiple fluorite-layered defects, disordered intergrowths $[Ln_3BaFeCuO_9]_m$ $[Ln_2BaFeCuO_7]_n$ *(Ln = Nd, Ce).* An original type of defect, observed for the first time, is shown in Fig. 7a. The Ba, Nd, and Ce positions are highlighted in this image, leading to the typical double rows and single rows of white dots. Two defects (arrowed) are observed where the double rows of white dots are replaced by triple rows and the adjacent layers are not shifted. These defective slices are interpreted by the introduction of an additional $[LnO_2]_\infty$ row at the level of the fluorite layers, leading to the formation of triple fluorite layers (TF) (Fig. 7b), i.e., to the local composition $Ln_3BaFeCuO_9$. Thus it appears that the possibility of synthesizing this latter structure, as well as intergrowths with general formula $[Ln_3BaFeCuO_9]_m$ $[Ln_2BaFeCuO_7]_n$ should be considered.

It is also worth pointing out that on the edges of the crystals, when parallel to the layers, larger multiple $(LnO_2)_p$ slices are frequently observed for $p = 4$ or 5 (Fig. 8), leading to local compositions $Ln_4BaFeCuO_{11}$ and $Ln_5BaFeCuO_{13}$. Moreover, it can be seen that in such areas the two types of layers, P and F, are easily connected. On the top of the image (Fig. 8a), a large fluorite slice is observed, coating the crystal edge; on both sides of the crystal (arrowed) two fluorite layers $[LnO_2]_2$ are connected to three $[(Cu, Fe)O_2][AO][(Cu, Fe)O_2]$ layers. The mismatch in the thickness of these layers is released on the edge of the crystal where the $[LnO_2]$ layers move more easily. The idealized model (Fig. 8b) shows that, in such a defect, the copper/iron atoms are inserted in the $[O_2]$ layers of the fluorite structure whereas a "superdislocation" mechanism is observed at the level of *Ln*–O layers.

(iii) Multiple perovskite-layered defects.

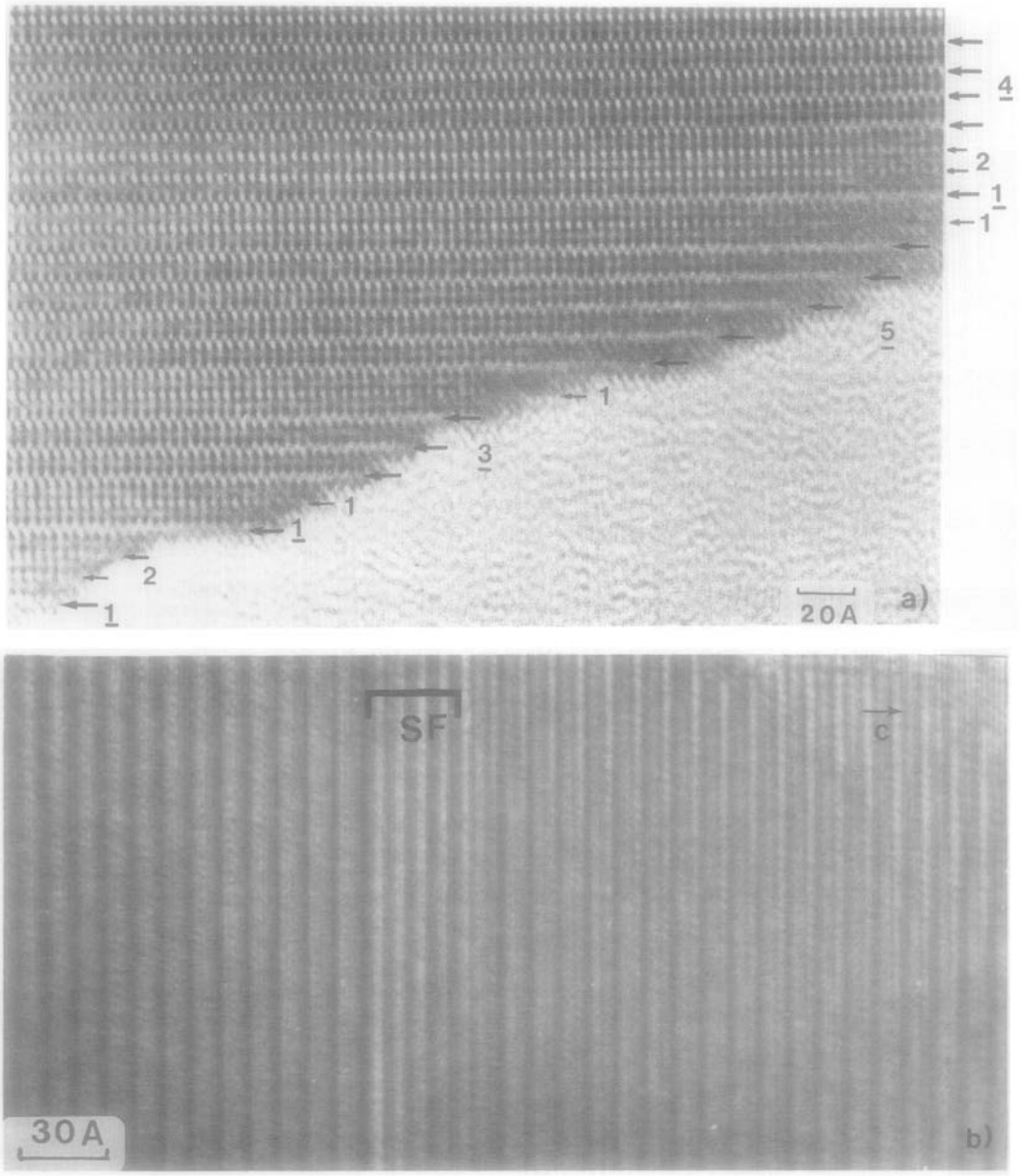

FIG. 6. (a) The defective SF layers are sometimes intergrown with double fluorite layers in aleatory sequences. The number of adjacent [$NdCeBaFeCuO_7$] type slices, indicated by large arrows, are underlined. The [$NdBaFeCuO_5$] type slices are marked by small arrows. (b) Four adjacent [NdBa $FeCuO_5$] slices observed in a regular crystal.

Extended defects corresponding to an increase in the thickness of the oxygen-deficient perovskite layers are also observed. An example is shown in Fig. 9; in this image the single rows of white dots are correlated with the $[BaO]_\infty$ layers. At the level of the defect (arrow (Fig. 9a)) a double row of barium layers is observed between the double

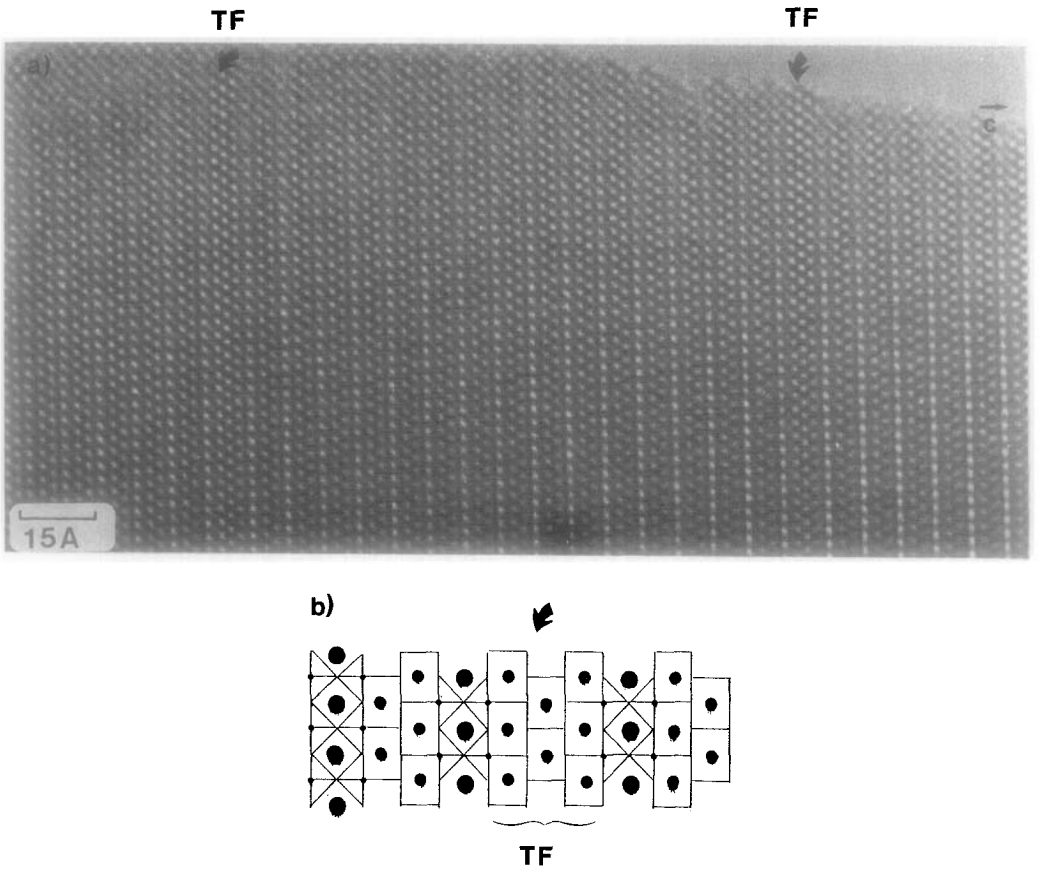

FIG. 7. (a) A [010] Image showing the existence of triple fluorite layers (TF). Note that the adjacent slices are not translated. (b) Ideal model, corresponding to a local composition $Ln_3BaFeCuO_9$.

fluorite layers. This defect corresponds to the replacement of a double copper/iron layer [$BaNdFeCuO_5$] (Fig. 2) by a triple oxygen-deficient perovskite copper/iron layer [$Ba_2Nd(Fe, Cu)_3O_{7+\delta}$] (Fig. 9b) similar to that encountered in the $YBa_2Cu_3O_7$ structure. Consequently, such defects associated with the matrix $BaLn_2FeCuO_7$ can be described as an intergrowth of the latter with the hypothetical $Ba_2Ln_2(Fe, Cu)_3O_{9+\delta}$ oxide according to the general formula $[Ba_2Ln_2(Fe, Cu)_3O_{9+\delta}]_m[BaLn_2FeCuO_7]_n$. It is worth pointing out that the limit member, which corresponds to $n = 0$ (i.e., $m = \infty$) has already been synthesized for the oxide $(Ln_{1-x}Ce_x)_2$ $(Ba_{1-y}Ln_y)_2Cu_3O_9$ (*5*, *6*); its structure consists of double fluorite-type layers interleaved between triple oxygen-deficient perovskite layers of the "123" type.

More rarely, in some defective crystals obtained from the samples with nominal composition $BaNdCeFeCuO_7$, very large perovskite slices were observed in the matrix (Fig. 10a); the E.D. pattern (Fig. 10b) attests of the superimposition of a second orthorhombic lattice "$a_p \times 2a_p \times c$", whose basal plane (001) is parallel to the layers (Fig. 10c). The origin of the "$2a_p$" superstructure cannot be elucidated from this image. Nevertheless, the disappearance of the contrast characteristic of the oxygen

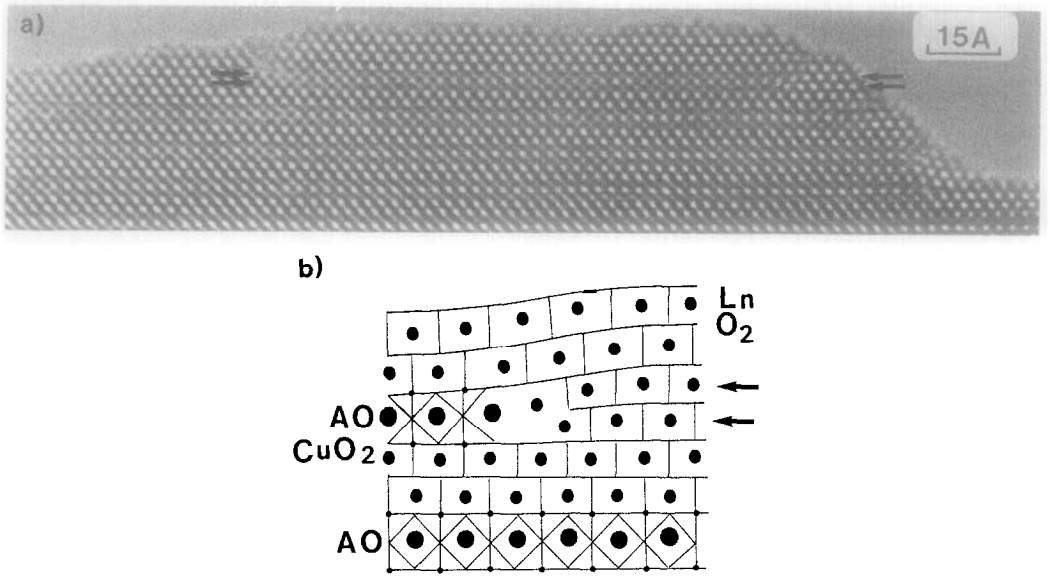

FIG. 8. (a) Large fluorite slices can be observed on the crystal edges. They are always easily connected to the perovskite layers. (b) Idealized model of the fluorite–perovskite layers connection.

free $[Nd]_\infty$ layers and the periodicity suggest that such perovskite layers contain more oxygen than those of the $NdBaFeCuO_5$ structure (Fig. 10d), perhaps due to a higher iron and neodymium content and to a higher oxidation state of iron, according to the formula $Ba_{0.5-y}Ln_{0.5+y}Fe_{0.5+x}Cu_{0.5-x}O_{3-\delta}$ in agreement with the existence of the oxide $NdBaFe_2O_{5.8}$ (*10*).

(*iv*) *Other complex extended defects.* The great adaptability of the fluorite and perovskite structures is also demonstrated by the existence of more complex extented defects. This is the case of the defect shown

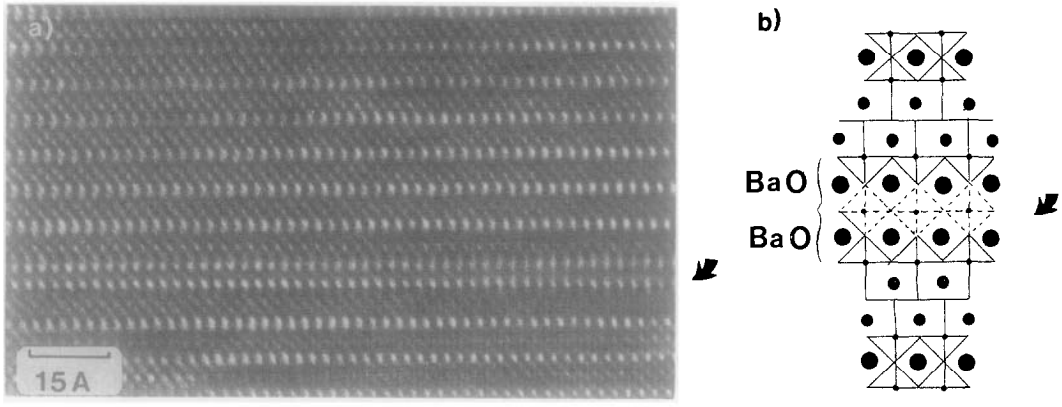

FIG. 9. (a) A [010] image where the $[BaO]_\infty$ layers appear as rows of white dots. A double row (arrowed) of white dots is observed, implying the existence of a triple copper/iron layer. (b) Idealized model of the defect.

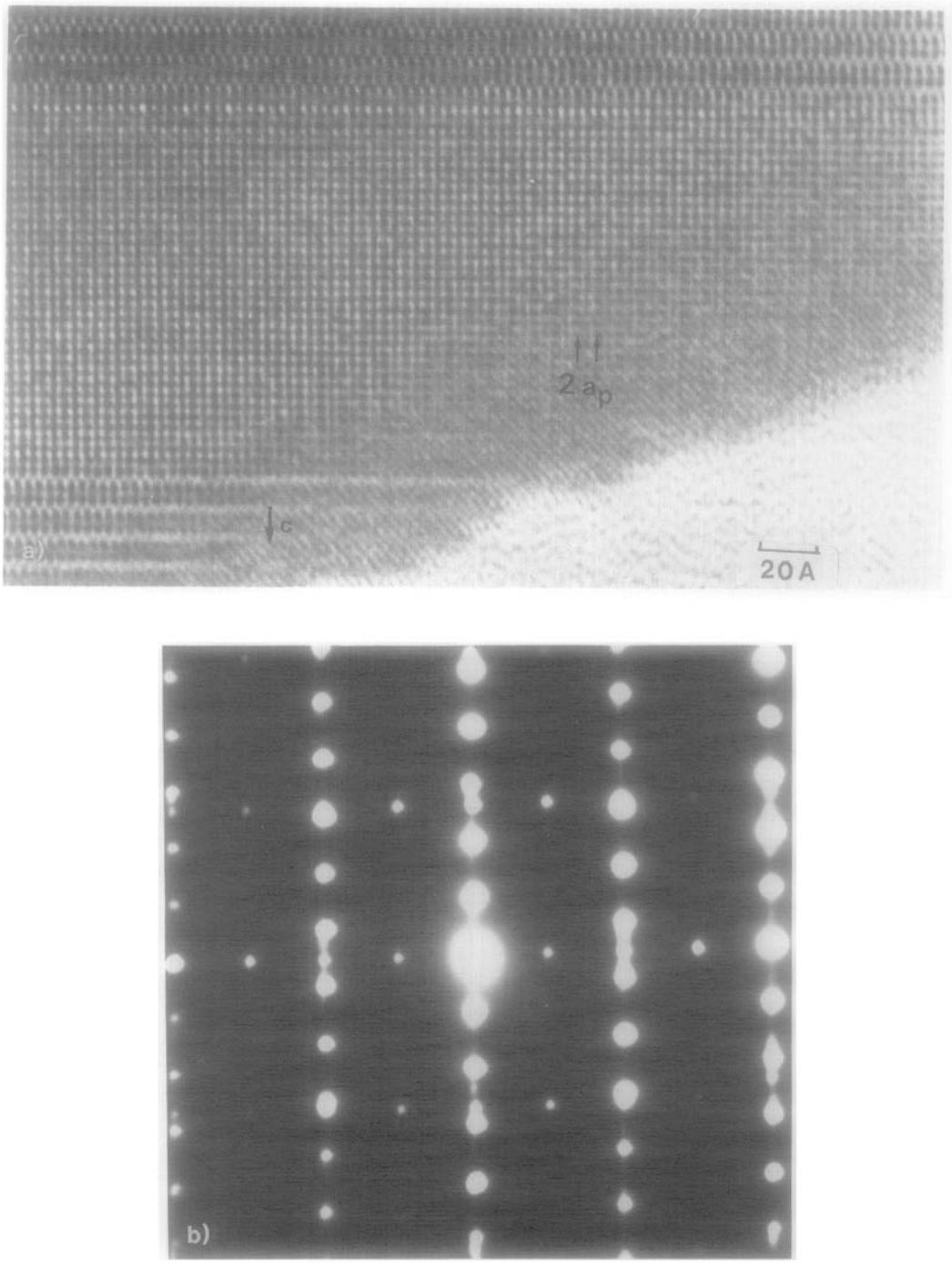

FIG. 10. (a) Example of a large perovskite layer (m = 31) in $BaNdCeFeCuO_7$. (b) Corresponding E.D. pattern showing the superposition of the two networks: $NdCeBaFeCuO_7$ and perovskite. (c) Representation of the two networks. Black dots correspond to the $NdCeBaFeCuO_7$ lattice (with $h + l = 2n$). Stars correspond to the second lattice with $a \sim a_p$ and $b \sim 2\ a_p$. The $A_\star$ and $C_\bullet$ axes are parallel. (d) Relative orientation of both lattices. The polyhedra of the perovskite structure (starred) can be octahedra, pyramids or tetrahedra.

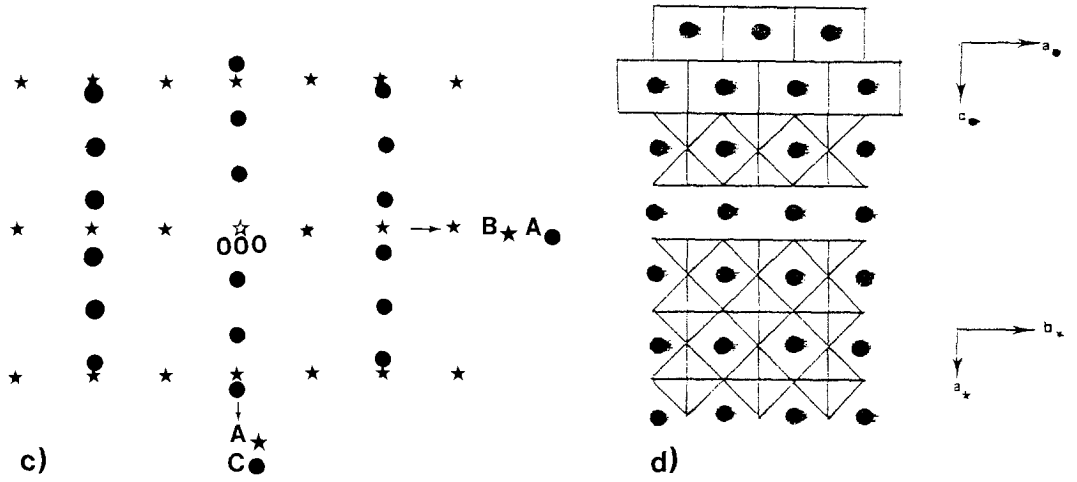

FIG. 10—*Continued*

in Fig. 11a which corresponds to a double superdislocation: simultaneously at almost the same level, a double *Ln* layer is replaced by a single one whereas the opposite mechanism is observed in the adjacent slices, so that the thickness of the four adjacent slices is preserved. It should be noted that the local thickness difference is ensured through an ondulation of the intermediate layer (arrows in Figs. 11a and 11b). Other sorts of superdislocation were observed at the level of the perovskite layer; an example is shown in Fig. 12 which can be interpreted as the elimination of one $[(Cu,Fe)O]_\infty$ layer in a triple copper/iron-layered defect $[Ba_2Ln_2(Fe, Cu)_3O_9]$ leading to a double copper/iron-layered defect $[BaNdFeCuO_5]_\infty$.

Concluding Remarks

From these results it is now possible to

TABLE III

STRUCTURAL FILIATIONS: THE TRIPLE INTERGROWTHS $[A_2Cu_2O_5]_h^P[A'CuO_{3-x}]_i^P[LnO_2]_j^F[A'O]_k^{RS}$ ARE DEDUCED FROM THE MOTHER STRUCTURES $[A_2Cu_2O_5]_h^P[A'CuO_{3-x}]_i^P[A'O]_k^{RS}$

Mother structures (MS)	Ideal 1–1 intergrowth of MS with CeO_2 fluorite	Experimental results	
$YBaFeCuO_5$ or $NdBaFeCuO_5$	$NdCeBaFeCuO_7$	$NdCe_{0.9}BaFe_{1.1}Cu_{0.9}O_7$ (this work)	$k = 0$ $i = 0$
$YBa_2Cu_3O_7$ or $NdBa_2Cu_3O_7$	$NdCeBa_2Cu_3O_9$	$(Ln_{1-x}Ce_x)_2(Ba_{1-y}Ln_y)_2Cu_3O_9$ (*5, 6*)	$k = 0$ $i = 1$
$Bi_2Sr_2CaCu_2O_8$ or $Tl_2Ba_2CaCu_2O_8$	$Bi_2Sr_2CaCeCu_2O_{10}$ or $Tl_2Ba_2CaCeCu_2O_{10}$	$Bi_2Sr_2Ln_{2-x}Ce_xCu_2O_{10}$ (Ln = Sm, Eu, Gd) $Tl_2Ba_2Ln_{2-x}Ce_xCu_2O_{10}$ (*3*)	$k = 3$ $i = 0$
$TlSr_2CaCu_2O_7$ or $TlBa_2CaCu_2O_7$	$TlSr_2CaCeCu_2O_9$ or $TlBa_2CaCeCu_2O_9$	$Tl_{1+x}A_{2-y}Ln_2Cu_2O_9$ (*1*) (Ln = Pr, Nd, Ce and A = Sr, Ba)	$k = 2$ $i = 0$
$La_2SrCu_2O_6$ or $Nd_2SrCu_2O_6$	$La_2SrCeCu_2O_8$ or $Nd_2SrCeCu_2O_8$	$Nd_{2.64}Sr_{0.82}Ce_{0.54}Cu_2O_8$ (T*) (*2*)	$k = 1$ $i = 0$
$Pb_2Sr_2Ca_{0.5}Y_{0.5}Cu_3O_8$	$Pb_2Sr_2Ca_{0.5}Y_{0.5}CeCu_3O_{10}$	$Pb_2Sr_2LnCeCu_3O_{10+\delta}$ (*4*)	$k = 2$ $i = 1$

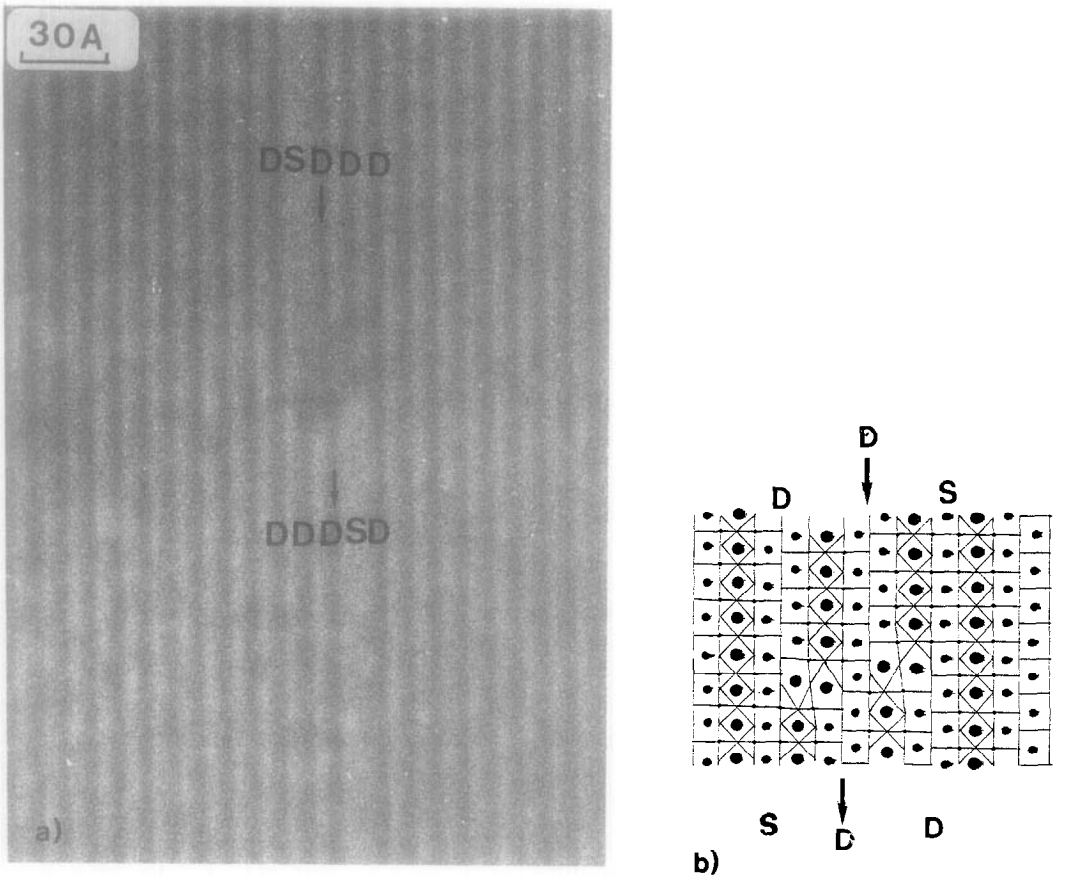

FIG. 11. (a) Example of extended defects corresponding to the existence of double superdislocations. D and S indicate the presence of double or single fluorite layers, respectively, sandwiched between double pyramidal layers. (b) Idealized model of such a defect.

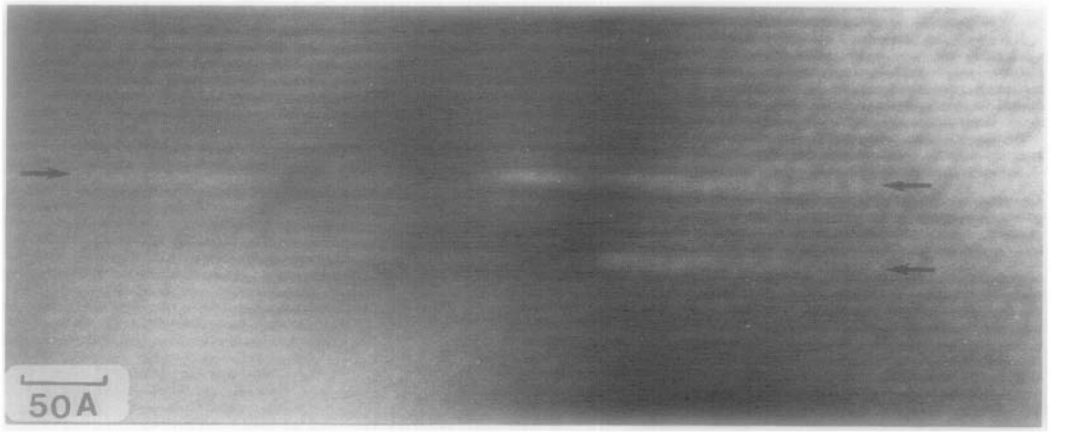

FIG. 12. Example of another type of superdislocation. On the right part of the image, two defective layers (arrowed) are observed corresponding to the existence of triple copper layers (periodicity ~14 Å). On the left part, only one defective slice is observed.

predict the possible existence of triple intergrowths between fluorite (F), perovskite (P), and rock salt (RS) structures according to the general formula $[A_2Cu_2O_5]^{P}_{h}[ACuO_{3-x}]^{P'}_{i}[LnO_2]^{F}_{j}[A'O]^{RS}_{k}$.

The structure of these oxides is derived from the mother structures (MS) observed for superconductive oxides $[A_2Cu_2O_5]^{P}_{h}[ACuO_{3-x}]^{P}_{i}[A'O]^{RS}_{k}$ by introduction of additional $[LnO_2]_\infty$ fluorite layers within $[A_2Cu_2O_5]_\infty$ double pyramidal copper layers. Thus, the existence of two consecutive pyramidal layers, the $[A_2Cu_2O_5]_\infty$ units ($h = 1$) (Fig. 1), appears absolutely necessary for the formation of such intergrowths. Table III summarizes the triple intergrowths which have been synthesized up to now. They all correspond to $h = j = 1$, whereas k ranges from 0 to 3. Many ordered and disordered intergrowths corresponding to the preceding observed defects can be expected.

References

1. C. Martin, D. Bourgault, M. Hervieu, C. Michel, J. Provost, and B. Raveau, *Modern Phys. Lett. B* **3,** 993 (1989).
2. J. Akimitsu, S. Suzuki, M. Watanabe, and H. Sawa, *Jpn. J. Appl. Phys.* **27,** L 1859 (1988).
3. Y. Tokura, T. Arima, H. Takagi, S. Uchida, T. Ishigaki, H. Asano, R. Bayers, A. I. Nazzal, P. Lacorre, and J. B. Torrance, *Nature* **342,** 890 (1989).
4. T. Rouillon, D. Groult, M. Hervieu, C. Michel, and B. Raveau, *Physica C* **167,** 107 (1990).
5. H. Sawa, K. Ohara, J. Akimitsu, Y. Matsui, and S. Horiuchi, *J. Phys. Soc. Jpn.* **58,** 2252 (1989).
6. T. Wada, A. Ichinose, Y. Yaegashi, H. Yamanchi, and S. Tanaka, *Phys. Rev. B* **41,** 1984 (1990).
7. L. Er-Rakho, C. Michel, Ph. Lacorre, and B. Raveau, *J. Solid State Chem.* **73,** 531 (1988).
8. D. B. Wiles and R. A. Young, *J. Appl. Cryst.* **14,** 149 (1981).
9. See for example for a review of the structure of superconducting cuprates: K. Yvon and M. François, *Z. Phys. B* **76,** 413 (1989).
10. L. Er-Rakho, Thesis, University of Caen, October 1987.